

Structure Formation, Backreaction and Weak Gravitational Fields

Aseem Paranjape* and T. P. Singh[†]

*Tata Institute of Fundamental Research,
Homi Bhabha Road,
Mumbai 400005, INDIA.*

Abstract

There is an ongoing debate in the literature as to whether the effects of averaging out inhomogeneities (“backreaction”) in Cosmology can be large enough to account for the acceleration of the scale factor in the FLRW models. In particular, some simple models of structure formation studied in the literature seem to indicate that this is indeed possible, and it has also been suggested that the perturbed FLRW framework is no longer a good approximation during structure formation, when the density contrast becomes nonlinear. In this work we attempt to clarify the situation to some extent, using a fully relativistic model of pressureless spherical collapse. We find that whereas averaging during structure formation can lead to acceleration via a selective choice of averaging domains, the acceleration is not present when more generic domains are used for averaging. Further, we show that for most of the duration of the collapse, matter velocities remain small, and the perturbed FLRW form of the metric can be explicitly recovered, in the structure formation phase. We also discuss the fact that the magnitude of the average effects of inhomogeneities depends on the scale of averaging, and while it may not be completely negligible on intermediate scales, it is expected to remain small when averaging on suitably large scales.

1 Introduction

Understanding the origin of Dark Energy is undoubtedly one of the most important problems in cosmology today. Recently, several workers in the field (including the present authors) [1, 2, 3, 4], have supported the hypothesis that the acceleration of the scale factor in the standard Friedmann-Lemaître-Robertson-Walker (FLRW) cosmologies, might be attributed to the effects of averaging over inhomogeneities in the real Universe. It is known that explicit averaging of the Einstein equations leads to non-trivial corrections [5, 6, 7]. These corrections or “backreaction”, it is argued, can mimic a Dark Energy term in the Cosmological equations. Specifically, some simple models have been presented which demonstrate how such an effect may arise [1].

On the other hand, it has also been argued that as long as the standard perturbed FLRW picture for the metric of the Universe is a good approximation, any effects of averaging over the inhomogeneous perturbations must remain small (see, e.g. Refs. [8, 9, 10, 11]). The counter given to this argument is that the perturbed FLRW framework is expected to break down around the time of structure formation [1]. That N -body simulations do not demonstrate any such breakdown is attributed to the fact that these simulations always work in the Newtonian limit of General Relativity (GR), usually employing periodic boundary conditions, and that

*E-mail: aseem@tifr.res.in

[†]E-mail: tpsingh@tifr.res.in

the backreaction due to averaging under such conditions can be shown to vanish [12]. Further, since the evolution of the background scale factor is fixed in the simulations, backreaction effects would not be visible even if present.

This situation clearly demands some clarification. One expects that as long as gravitational fields are weak, the perturbed FLRW framework should work well. Is the weak field approximation then actually breaking down during structure formation? If so, then clearly a radical rethink of the approach to Cosmology is in order. If not, on the other hand, then one needs to understand how simple models such as the one presented by Räsänen [1] can achieve an acceleration upon averaging during structure formation.

In this paper we will attempt to address these issues. We employ a simple but fully relativistic model of spherical collapse, *with appropriate initial conditions imposed*. We will show that the effect observed by Räsänen can actually be attributed to a very selective choice of averaging domain, and that in fact the effect is not present when a more generic averaging domain is chosen. However, we do find that the effect of averaging inhomogeneities may not be completely negligible. In particular we see $\sim 10\%$ deviations of the effective deceleration parameter to be defined below, from the expected FLRW value, on the scale over which we define our averaged quantities. This is in line with the findings of Li and Schwarz [13, 14] in the context of averaging of perturbative inhomogeneities. To support these results, we will show that at any stage of the collapse, *if matter velocities are small*, then the weak field conditions hold and one can explicitly recover the perturbed FLRW form of the metric. We will see that matter velocities do, in fact, remain small for most of the duration of the collapse. We will also present an argument explaining the origin of the $\sim 10\%$ effect from perturbative metric inhomogeneities on the scales at hand, and argue that in the real universe, the averaging scale is expected to be large enough for these effects to be much smaller.

We have organised the paper as follows. In section 2 we will set up our model for the spherical collapse, and compare its results with those obtained by Räsänen. In section 3 we will show how the perturbed FLRW metric is recovered, and we will conclude in section 4 with a discussion of further tests of the backreaction argument.

2 Spherical Collapse : Setting up the model

Before we describe the model we use, it will help to recall the model used by Räsänen [1], which is what we wish to compare with. Räsänen’s model can be summarized as follows : one considers two disjoint regions, one overdense and the other completely empty, each evolving according to the FLRW evolution equations. (The embedding of these regions in an FLRW background, and the behaviour of the region *between* these two regions, is not considered.) The scale factor in the overdense region therefore behaves as $a_1 \propto (1 - \cos u)$ with $t \propto (u - \sin u)$, and the scale factor in the empty region behaves as $a_2 \propto t$. It is then straightforward to show that if one defines a volume averaged scale factor by $a^3 \equiv a_1^3 + a_2^3$, then the effective deceleration parameter given by $q \equiv -(\ddot{a}a)/\dot{a}^2$ becomes negative (indicating acceleration) around the time that the overdense region turns around and starts collapsing. In what follows, we will attempt to reconstruct such a situation more rigorously, with appropriate matching and initial conditions taken care of.

2.1 The LTB solution

We will employ a model containing spherically symmetric pressureless “dust”, with the energy-momentum tensor given by

$$T_{ab} = \text{diag}(\rho(t, r), 0, 0, 0). \quad (1)$$

The line element of interest is hence the Lemaître-Tolman-Bondi (LTB) metric [17] given in synchronous and comoving coordinates, by

$$ds^2 = -dt^2 + \frac{R'^2 dr^2}{1 - k(r)r^2} + R^2 d\Omega^2, \quad (2)$$

where $R(t, r)$ is the area radius of a shell of matter labelled by the comoving radius r , and $k(r)$ is a function of integration to be determined by the initial conditions. (A prime and a dot refer to derivatives with respect to r and t respectively. We set the speed of light $c = 1$, except when displaying numerical results where we will explicitly account for factors of c .) The equations of motion are

$$\dot{R}^2 = \frac{2GM(r)}{R} - k(r)r^2, \quad (3)$$

$$\rho(t, r) = \frac{M'(r)}{4\pi R^2 R'}, \quad (4)$$

where $M(r)$ is another function of integration which can be determined from the initial density profile once a scaling freedom in the coordinate r is fixed. The spherical collapse model has been extensively studied in the literature in the context of structure formation [18]. However, to the best of our knowledge, the issue of whether or not the collapse situation can be recast as perturbed FLRW, has not been discussed.

The solutions to Eqn. (3) depend on the sign of the function $k(r)$, and can be given in parametric form as

$$R(r, t) = \left(\frac{9GM(r)}{2} \right)^{1/3} (t - t_s(r))^{2/3}, \quad \text{for } k(r) = 0, \quad (5a)$$

$$R = \frac{GM(r)}{-k(r)r^2} (\cosh \eta - 1) \quad ; \quad t - t_s(r) = \frac{GM(r)}{(-k(r)r^2)^{3/2}} (\sinh \eta - \eta), \quad 0 \leq \eta < \infty, \quad \text{for } k(r) < 0, \quad (5b)$$

$$R = \frac{GM(r)}{k(r)r^2} (1 - \cos \eta) \quad ; \quad t - t_s(r) = \frac{GM(r)}{(k(r)r^2)^{3/2}} (\eta - \sin \eta), \quad 0 \leq \eta \leq 2\pi, \quad \text{for } k(r) > 0. \quad (5c)$$

The function $t_s(r)$ appearing above is completely determined once $k(r)$ and $M(r)$ are known and a scaling choice for r is made. Since we will always start the evolution at $t = t_i > t_s(r)$, this function will be of little physical relevance, except to ensure consistency at $t = t_i$.

2.2 Initial conditions

While choosing the initial density, velocity and coordinate scaling profiles, we make the important assumption that at initial time, a well-defined *global* background FLRW solution can be identified, with scale factor $a(t)$, Hubble parameter $H(t)$ and density $\bar{\rho}(t)$. This is reasonable since the CMB data (combined with the Copernican principle) assure us that inhomogeneities at the last scattering epoch were at the level of 10 parts per million. This assumption plays a crucial role in deciding which regions are overdense and will eventually collapse, and which regions will keep expanding (see also the first paper in Ref. [4] for a discussion on this point).

- **Initial density profile $\rho(t_i, r)$:**

The initial density is chosen to be

$$\rho(t_i, r) = \bar{\rho}_i \begin{cases} (1 + \delta_*), & r < r_* \\ (1 - \delta_v), & r_* < r < r_v \\ 1, & r > r_v, \end{cases} \quad (6)$$

where $\bar{\rho}_i = \bar{\rho}(t_i)$. Initially, the region $r < r_*$ is assumed to contain a tiny overdensity and the region $r_* < r < r_v$, an underdensity. In other words,

$$0 < \delta_*, \delta_v \ll 1. \quad (7)$$

The discontinuities in the initial density profile can be smoothed out by replacing the step functions appropriately. We will not do this here, since the step functions make calculations very simple. This is not expected to affect the qualitative features of our final results.

- **Initial conditions on scaling and velocities :**

We match the initial velocity and coordinate scaling to the global background solution, by requiring

$$R(t_i, r) = a_i r, \quad (8)$$

$$\dot{R}(t_i, r) = a_i H_i r, \quad (9)$$

with a_i and H_i denoting the initial values of the scale factor and Hubble parameter respectively of the global background. This amounts to setting the initial velocities to match the Hubble flow, ignoring initial peculiar velocities. This is only a convenient choice and the introduction of initial peculiar velocities is not expected to modify our final results qualitatively.

For the FLRW background we consider an Einstein-deSitter (EdS) solution with scale factor and Hubble parameter given by

$$a(t) = (t/t_0)^{2/3} \quad ; \quad t_0 = 2/(3H_0), \quad (10)$$

$$H(t) \equiv \dot{a}/a = 2/(3t), \quad (11)$$

with t_0 denoting the present epoch. a_i fixes the initial time as

$$t_i = 2/(3H_0)a_i^{3/2}. \quad (12)$$

We will always use $a_i = 10^{-3}$, so that the initial conditions are being set around the CMB last scattering epoch; in general a_i must be treated as one of the parameters in the problem. The initial EdS background density is given in terms of H_0 and a_i as

$$\bar{\rho}_i = \frac{3}{8\pi G} H_0^2 a_i^{-3}. \quad (13)$$

2.3 Mass function $M(r)$ and curvature function $k(r)$

We now have enough information to fix $M(r)$ and $k(r)$. Using Eqn. (4) at initial time together with the scaling in Eqn. (8) gives us

$$GM(r) = \frac{1}{2} H_0^2 r^3 \begin{cases} 1 + \delta_*, & 0 < r < r_* \\ 1 + \delta_v \left((r_c/r)^3 - 1 \right), & r_* < r < r_v \\ 1 + (\delta_v/r^3) (r_c^3 - r_v^3), & r > r_v, \end{cases} \quad (14)$$

where we have defined a “critical” radius r_c by the equation

$$\left(\frac{r_c}{r_*} \right)^3 = 1 + \frac{\delta_*}{\delta_v}. \quad (15)$$

The significance of r_c will become apparent shortly. Using the initial conditions Eqns. (8) and (9) in the evolution equation (3) at initial time, gives

$$k(r)r^2 = \frac{2GM(r)}{a_i r} - a_i^2 H_i^2 r^2, \quad (16)$$

with $H_i^2 = H_0^2 a_i^{-3}$, and hence

$$k(r) = \frac{H_0^2}{a_i} \begin{cases} \delta_*, & r < r_* \\ \delta_v \left((r_c/r)^3 - 1 \right), & r_* < r < r_v \\ (\delta_v/r^3) (r_c^3 - r_v^3), & r > r_v. \end{cases} \quad (17)$$

The significance of r_c is now clarified. Since $\delta_*, \delta_v > 0$, we have $r_c > r_*$ by definition (Eqn. (15)). The following possibilities arise :

- If $r_c > r_v$, then $k(r) > 0$ for all r , and every shell will ultimately collapse, including the “void” region $r_* < r < r_v$.
- If $r_c < r_v$, then $k(r) > 0$ for $r < r_c$ and changes sign at $r = r_c$. Hence, the region $r_* < r < r_c$ will collapse even though it is underdense, while the region $r > r_c$ will expand forever.
- If $r_c = r_v$, then the “void” exactly compensates for the overdensity, and the universe is exactly EdS for $r > r_v$. [$GM(r) = (1/2)H_0^2 r^3$ and $k(r) = 0$.] Also the “void” will eventually collapse.

Clearly the most interesting case for us is the one with $r_c < r_v$, and we will hence make this choice for our model. We realize that the model as it stands is not a very realistic depiction of the (nearly spherical) voids we see in our Universe [15], since these voids are seen to be *surrounded* by “walls” of matter. However, our goal is to describe two regions, one of which collapses while the other expands ever more rapidly, and our model is capable of doing so while retaining its fully relativistic character.

Although we have set up the model for all values of the radial coordinate r , hereon we will concentrate on the region $0 < r < r_v$. One reason is that most of the interesting dynamics takes place in this region. Another is that the region $r > r_v$ develops shell-crossing singularities due to the sharp rise in density across $r = r_v$. A more realistic model would be able to incorporate the pressures that are expected to build up when a shell-crossing occurs ([16], see also the discussion in section 4 below), but the LTB model is limited in this respect due to its pressureless character. We will therefore ignore the region $r > r_v$.

2.4 The solution in the region $0 < r < r_v$

The region of interest can be split into three parts : Region 1 = $\{0 < r < r_*\}$, Region 2 = $\{r_* < r < r_c\}$ and Region 3 = $\{r_c < r < r_v\}$. The solution in the three regions is as follows :

- **Region 1** ($0 < r < r_*$) :

$$R = \frac{1}{2} \left(\frac{a_i}{\delta_*} \right) r (1 + \delta_*) (1 - \cos u), \quad (18a)$$

$$u - \sin u = \frac{2H_0}{1 + \delta_*} \left(\frac{\delta_*}{a_i} \right)^{3/2} (t - t_i) + (u_i - \sin u_i), \quad (18b)$$

$$1 - \cos u_i = \frac{2\delta_*}{1 + \delta_*}, \quad (18c)$$

$$R^2 R' = \frac{R^3}{r}. \quad (18d)$$

For Regions 2 and 3, it is convenient to define a function $\varepsilon(r)$ as

$$\varepsilon(r) \equiv \delta_v \left(\left(\frac{r_c}{r} \right)^3 - 1 \right) = \frac{a_i}{H_0^2} k(r), \quad r_* < r < r_v. \quad (19)$$

• **Region 2** ($r_* < r < r_c$) :

$$R = \frac{1}{2} \left(\frac{a_i}{\varepsilon} \right) r (1 + \varepsilon) (1 - \cos \alpha), \quad (20a)$$

$$\alpha - \sin \alpha = \frac{2H_0}{1 + \varepsilon} \left(\frac{\varepsilon}{a_i} \right)^{3/2} (t - t_i) + (\alpha_i - \sin \alpha_i), \quad (20b)$$

$$1 - \cos \alpha_i(r) = \frac{2\varepsilon}{1 + \varepsilon}, \quad (20c)$$

$$R^2 R' = \frac{R^3}{r} \left(1 - \frac{r\varepsilon'}{\varepsilon(1 + \varepsilon)} \left\{ 1 - \frac{\varepsilon^{3/2}}{(1 - \cos \alpha)^2} \left[H_i(t - t_i) \sin \alpha \left(\frac{3 + \varepsilon}{1 + \varepsilon} \right) + \frac{4\varepsilon^{1/2}}{(1 + \varepsilon)^2} \left(\frac{\sin \alpha}{\sin \alpha_i} \right) \right] \right\} \right). \quad (20d)$$

• **Region 3** ($r_c < r < r_v$) :

$$R = \frac{1}{2} \left(\frac{a_i}{|\varepsilon|} \right) r (1 + \varepsilon) (\cosh \eta - 1), \quad (21a)$$

$$\sinh \eta - \eta = \frac{2H_0}{1 + \varepsilon} \left(\frac{|\varepsilon|}{a_i} \right)^{3/2} (t - t_i) + (\sinh \eta_i - \eta_i), \quad (21b)$$

$$\cosh \eta_i(r) - 1 = \frac{2|\varepsilon|}{1 + \varepsilon}, \quad (21c)$$

$$R^2 R' = \frac{R^3}{r} \left(1 - \frac{r\varepsilon'}{\varepsilon(1 + \varepsilon)} \left\{ 1 - \frac{|\varepsilon|^{3/2}}{(\cosh \eta - 1)^2} \left[H_i(t - t_i) \sinh \eta \left(\frac{3 + \varepsilon}{1 + \varepsilon} \right) + \frac{4|\varepsilon|^{1/2}}{(1 + \varepsilon)^2} \left(\frac{\sinh \eta}{\sinh \eta_i} \right) \right] \right\} \right). \quad (21d)$$

The crossover from Region 1 to Region 2 is discontinuous in R' (but not in R) due to our discontinuous choice of initial density. Smoothing out the density will also smooth out R' . The crossover from Region 2 to Region 3 can be shown to be smooth, by considering the limits $r \rightarrow r_c^-$ and $r \rightarrow r_c^+$ or equivalently $\varepsilon \rightarrow 0^-$ and $\varepsilon \rightarrow 0^+$. Note that the results in Eqns. (18), (20) and (21) are exact, and do not involve any perturbative expansions in δ_* or δ_v , even though these parameters are small.

2.5 Behaviour of the model

Each shell in the inner, homogeneous and overdense Region 1 behaves as a closed FLRW universe, expanding out to a maximum radius $R_{max}(r)$ given by

$$R_{max}(r) = \frac{a_i}{\delta_*} r (1 + \delta_*). \quad (22)$$

All the inner shells reach their maximum radius and turn around at the same time t_{turn} given

Parameter name	Parameter value
a_i	0.001
H_0	$1/13.59 \text{ Gyr}^{-1}$ ($= 72 \text{ km/s/Mpc}$)
t_0	$2/(3H_0) = 9.06 \text{ Gyr}$
c	$306.6 \text{ MpcGyr}^{-1}$
δ_*	$1.25a_i(3\pi/4)^{2/3} = 2.21 \times 10^{-3}$
δ_v	0.005
r_*	$0.004c/H_0 = 16.7 \text{ Mpc}$
t_{turn}/t_0	0.72
r_c	$r_*(1 + \delta_*/\delta_v)^{1/3} = 18.8 \text{ Mpc}$
r_v	$1.25r_c = 23.5 \text{ Mpc}$
$R(t_0, r_*)$	6.8 Mpc
$R(t_0, r_v)$	33.3 Mpc

Table 1: Values of various parameters used in generating plots.

by

$$t_{turn} = t_i + \frac{1 + \delta_*}{2H_0} \left(\frac{a_i}{\delta_*} \right)^{3/2} (\pi - (u_i - \sin u_i)) \approx t_0 \left(\frac{3\pi}{4} \right) \left(\frac{a_i}{\delta_*} \right)^{3/2}, \quad (23)$$

where we have used the smallness of a_i and δ_* to make the last approximation. By appropriately choosing a value of δ_* , we can arrange for the turnaround of Region 1 to occur either before or after the present epoch.

In Table 1 we have listed the parameter values which we will use frequently in displaying plots. Along with the parameter set $\{a_i, H_0, \delta_*, \delta_v, r_*, r_v\}$, we have also listed the values of the derived quantities $\{r_c, t_i, t_0, t_{turn}\}$ and speed of light c in units of MpcGyr^{-1} . We have also shown the values of the present day physical area radius $R(t_0, r)$ at $r = r_*$ and $r = r_v$. The density contrasts are to be understood to reflect the inhomogeneities in the dark matter density close to last scattering, and not the inhomogeneities of the baryons which were much smaller [19, 20].

In Fig. 1 we have shown the evolution of the density contrast $\delta(t, r)$ defined in the usual way by

$$1 + \delta(t, r) = \frac{\rho(t, r)}{\bar{\rho}(t)}, \quad (24)$$

for the parameter choices of Table 1, for which one has $t_{turn}/t_0 \simeq 0.72$, so that the collapse is well under way in Region 1 at the present epoch. The two panels show the contrast for two representative values of r , one in Region 1 and the other in Region 3.

For clarity, we define the volume of each of our three comoving regions separately, as

$$V_1 \equiv 4\pi \int_0^{r_*} \frac{R^2 R'}{\sqrt{1 - k(r)r^2}} dr \quad ; \quad V_2 \equiv 4\pi \int_{r_*}^{r_c} \frac{R^2 R'}{\sqrt{1 - k(r)r^2}} dr \quad ; \quad V_3 \equiv 4\pi \int_{r_c}^{r_v} \frac{R^2 R'}{\sqrt{1 - k(r)r^2}} dr. \quad (25)$$

The total volume of the region is used to define a volume averaged scale factor as

$$a(t) \equiv \left(\frac{V(t)}{V(t_0)} \right)^{1/3} \quad ; \quad V(t) \equiv V_1(t) + V_2(t) + V_3(t), \quad (26)$$

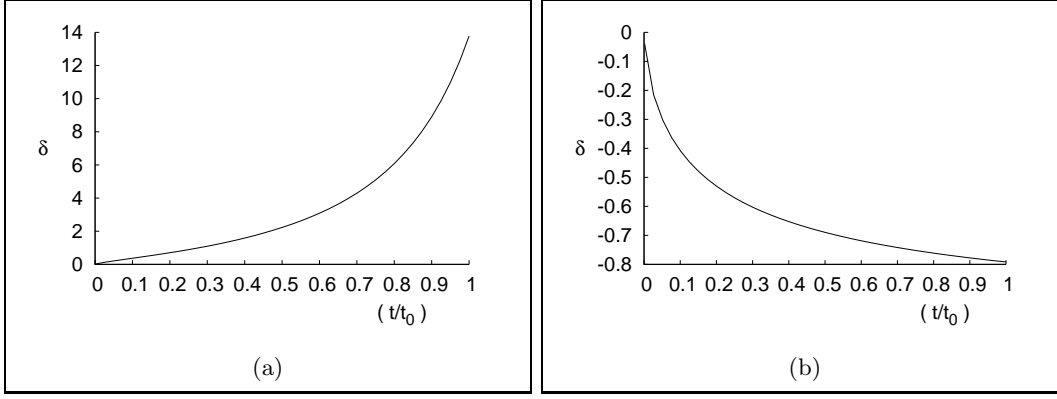


Figure 1: The evolution of the density contrast $\delta(t, r)$, using parameter values from Table 1 evaluated at (a) $r = r_*/2$ in Region 1 and (b) $r = (r_c + r_v)/2$ in Region 3.

and hence an effective deceleration parameter q given by

$$q \equiv -\frac{\ddot{a}a}{\dot{a}^2} = 2 - 3\frac{\ddot{V}V}{\dot{V}^2}. \quad (27)$$

On the other hand, we note that Räsänen’s model can be mimicked more closely by ours, if we simply remove the Region 2, by hand. By doing so we are left with two disjoint regions, each spherically symmetric, one of which is collapsing and the other expanding ever rapidly and becoming ever emptier. There is no physical reason to throw away Region 2 in this manner, but for the sake of comparison we will define a “modified” scale factor a_{mod} and its corresponding deceleration parameter q_{mod} by

$$a_{mod}(t) \equiv \left(\frac{V_1(t) + V_3(t)}{V_1(t_0) + V_3(t_0)} \right)^{1/3} ; \quad q_{mod} \equiv -\frac{\ddot{a}_{mod}a_{mod}}{\dot{a}_{mod}^2}. \quad (28)$$

Note that the normalisation of the scale factor is irrelevant in defining the deceleration parameter. In Fig. 2 we plot $q(t)$ and $q_{mod}(t)$, for several sets of initial conditions which are close to our “base set” listed in Table 1 (except for Fig. 2d which has a large value for δ_v)¹. The various integrals involved in computing $V(t)$, etc. were performed using the `NIntegrate` routine of *Mathematica*. To generate the plots we used the numerical derivative routine `ND` of *Mathematica*. The various initial conditions correspond to turnaround times that are slightly greater than, or slightly less than, or significantly less than the present epoch. The idea here is to demonstrate that the results are valid regardless of whether the collapse has just begun or is well under way at the present epoch. We see that while the modified scale factor does accelerate as in Räsänen’s model, the scale factor $a(t)$ which is the more natural choice in our situation, does not show this effect. The reason for this can be understood as follows. The Region 2 is of a rather peculiar nature – it is underdense initially and becomes emptier with time, however its evolution is closely linked to that of the *overdense* Region 1. Namely, the whole of Region 2 (except its boundary at $r = r_c$), is dragged along with Region 1 and eventually turns around, instead of expanding away to infinity like its counterpart Region 3. Now, if one ignores Region 2, then Räsänen’s arguments about the remaining two regions stand – one region is contracting and the other is expanding faster than the global mean, and this stand-off leads to an acceleration of the effective scale factor a_{mod} , as we see in the plots of Fig. 2. But if we account for Region 2 as well, then we bring in a counter-balancing influence of a large *underdense* volume

¹Both curves in Fig. 2d begin at $q \sim 0.5$ at $t = t_i$. To enhance the contrast between the curves, we have plotted them for times $t > 0.15t_{turn}$. The remaining plots (Figs. 2a–2c) are plotted starting from $t = t_i$.

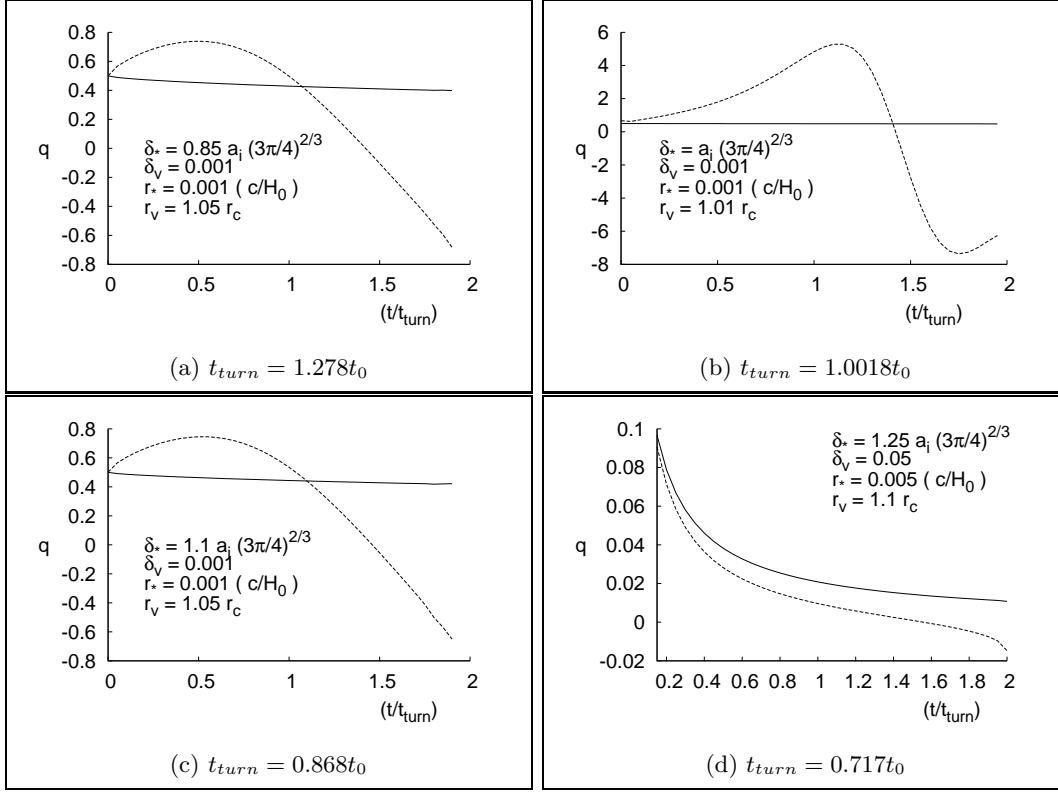


Figure 2: The deceleration parameters for a range of parameter values. The dashed lines correspond to q_{mod} and the solid lines to q . The x-axis shows t/t_{turn} , where t_{turn} is the time at which Region 1 turns around, and is different for each plot. The values for a_i , H_0 and c are the same as those listed in Table 1. [Both curves in Fig. 2d begin at $q \sim 0.5$ at $t = t_i$.]

which is expanding *slower* than average, and this reduces the accelerating influence of Region 3 to the point of making the effect completely disappear. Note that at late times, the volume of Region 1 contributes negligibly to the total volume, and the volumes of regions 2 and 3 are comparable.

The figures (2a)-(2c) show that while the full deceleration parameter q does not change sign, it does deviate from the EdS value of $(1/2)$, by an amount of the order of $\sim 10\%$. This indicates that while backreaction may not be large enough to cause the scale factor to accelerate, it may still lead to effects which are not completely negligible.

We wish to highlight two points. First, it is very important to note the role played by the initial conditions in this entire exercise. The function $k(r)$ is defined in a continuous fashion once the initial density, velocity and coordinate scaling are given, and $k(r)$ then decides which shells will eventually collapse and which will not. The continuity of $k(r)$ assures us that in models such as ours, with an overdensity surrounded by an underdensity, the underdense region *will always* contain a subregion in which $k(r) > 0$. We see therefore that the existence of Region 2, is a generic feature not restricted to our specific choice of discontinuous initial density or vanishing initial peculiar velocities. Further, as we see in Fig. 2d, it is possible to make q deviate even more significantly from the EdS value than the $\sim 10\%$ effect of the first three figures, but this requires an unnaturally high value of $\delta_v \gtrsim 0.01$ (the figure has $\delta_v = 0.05$), which contradicts CMB data.

Secondly, one may argue about the “naturalness” of choosing one set of regions over another set, in order to compute volumes. But this itself places the physicality of the acceleration effect into question – if one has to judiciously choose a specific set of averaging domains in order to

obtain acceleration on average, then the effect would appear to be an artifact of this choice rather than something which observers would see.

Having seen that the average behaviour of the full region $0 < r < r_v$ is close to EdS, we can ask whether one can explicitly show that the *metric* for this system is actually close to FLRW. We answer this in the affirmative in the next section.

3 Transforming to Perturbed FLRW form

We ask whether the metric (2) can be brought to the perturbed FLRW form with scalar perturbations, at any arbitrary stage of the collapse. Namely, we want a coordinate transformation $(t, r) \rightarrow (\tilde{t}, \tilde{r})$ such that the metric in the new coordinates is

$$ds^2 = -(1 + 2\tilde{A})d\tilde{t}^2 + a^2(\tilde{t})(1 + 2\tilde{\psi})(d\tilde{r}^2 + \tilde{r}^2 d\Omega^2), \quad (29)$$

with at least the conditions

$$|\tilde{A}| \ll 1 \quad ; \quad |\tilde{\psi}| \ll 1, \quad (30)$$

being satisfied. We will ignore conditions on the derivatives of $\tilde{\psi}$ and \tilde{A} for now (see the end of Section 3.2). The scale factor is the EdS solution, with \tilde{t} as the argument. The coordinate \tilde{r} is comoving with the (fictitious) background Hubble flow, but not with the matter itself. On physical grounds we expect that this transformation should be possible as long as the gravitational field is weak and matter velocity is small. We will see below that this is exactly what happens. In the new coordinates, all matter shells labelled by \tilde{r} expand with the Hubble flow, with a superimposed peculiar velocity.

Since we want \tilde{r} to be comoving with the background, the natural choice for this coordinate would be $\tilde{r} \sim R/a$, at least at early times. Also, we need to account for the local spatial curvature induced by the initial conditions. As an ansatz for the coordinate transformation therefore, we consider the equations

$$\tilde{r} = \frac{R(t, r)}{a(t)} (1 + \xi(t, r)), \quad (31a)$$

$$\tilde{t} = t + \xi^0(t, r), \quad (31b)$$

where $\xi(t, r)$ and $\xi^0(t, r)$ are expected to satisfy

$$|\xi| \ll 1 \quad ; \quad |\xi^0 H| \ll 1. \quad (32)$$

This form of the transformation keeps us close to the standard gauge transformation of cosmological perturbation theory, while still accounting for the deviations in the evolution from the background FLRW, caused by structure formation. We will show that a self-consistent transformation exists, which preserves the conditions (30) and (32) for most of the evolution. We will use the metric transformation rule given by

$$\tilde{g}_{ab}(\tilde{x}) \frac{\partial \tilde{x}^a}{\partial x^i} \frac{\partial \tilde{x}^b}{\partial x^j} = g_{ij}(x), \quad (33)$$

and *expand to leading order* in the small functions ξ , $\xi^0 H$, \tilde{A} , $\tilde{\psi}$ and also $k(r)r^2$ which, as we see from Eqn. (17), remains small in the entire region of interest. The relations in Eqn. (33) must be analysed for the cases $(ij) = \{(tt), (tr), (rr), (\theta\theta)\}$, in each of the three regions. (The remaining cases can be shown to lead to trivial or non-independent relations.) The analysis is similar to the standard gauge transformation analysis in relativistic perturbation theory [19]. Since the calculations involved are straightforward but tedious, we will only present an outline

of the calculation and highlight certain issues. At the end we will present equations for all three regions and numerically show that the transformation is well-behaved in the regime of interest.

The cases $(ij) = (\theta\theta)$ and (rr) are easily analysed and lead to

$$\tilde{\psi} = -\xi^0 H - \xi, \quad (34)$$

and

$$\xi' = \frac{1}{2}k(r)r^2 \left(\frac{R'}{R} \right). \quad (35)$$

The cases $(ij) = (tr)$ and (tt) both require $|\partial_t \tilde{r}| \ll 1$ for consistency (since the RHS of Eqn. (33) in these cases has no zero order term to balance a large $\partial_t \tilde{r}$). Note that since t is the proper time of each matter shell, the quantity $\partial_t \tilde{r}$ is simply the velocity of matter in the (\tilde{t}, \tilde{r}) frame (which is comoving with the Hubble flow). In other words,

$$\tilde{v} \equiv \frac{\partial \tilde{r}}{\partial t}, \quad (36)$$

is the radial comoving peculiar velocity of the matter shells in the (\tilde{t}, \tilde{r}) frame. We will soon see that whereas the quantities ξ and ξ^0 behave roughly as $\sim (H_0 r)^2$, the peculiar velocity $a\tilde{v}$ behaves roughly as $\sim (H_0 r)$. We will therefore treat $(a\tilde{v})^2$ as a small quantity of the same order as ξ , etc. The case $(ij) = (tr)$ then leads to

$$\xi^{0'} = a\tilde{v}R', \quad (37)$$

and the case $(ij) = (tt)$ gives

$$\tilde{A} = -\dot{\xi}^0 + \frac{1}{2}(a\tilde{v})^2. \quad (38)$$

The equations (34), (35), (37), and (38) are valid in the entire range $0 < r < r_v$, provided the peculiar velocity remains small in magnitude. The comoving peculiar velocity is given by

$$\tilde{v} = \partial_t \left(\frac{R}{a} \right), \quad (39)$$

where we have assumed for consistency that $|\partial_t(R/a)| \ll 1$ and have dropped the term $(R/a)\dot{\xi}$ since it is expected to be of higher order than $\partial_t(R/a)$. (This can be seen from simple dimensional considerations – we have $\partial_t(R/a) \sim HR/a$, and since, from Eqns. (35) and (17), $\xi \sim (HR)^2$, we also have $(R/a)\dot{\xi} \sim (HR)^3/a$.) We will see that these conditions do indeed hold for most of the evolution, throughout the region of interest.

3.1 The transformation in Region 1

Since Region 1 corresponds to a homogeneous solution, the integrals in Eqns. (35) and (37) can be analytically performed. Eqn. (35) directly gives

$$\xi = \frac{1}{4}k(r)r^2 = \frac{1}{4} \left(\frac{\delta_*}{a_i} \right) (H_0 r)^2, \quad (40)$$

after setting an arbitrary function of time to zero. Hence \tilde{v} has the structure $\tilde{v} = ry_1(t)$, since R has the structure $R = ry_2(t)$. Eqn. (37) then leads to

$$\xi^0 = \frac{1}{2}\tilde{v}aR, \quad (41)$$

after setting another arbitrary function of time to zero. [Note that it might be more meaningful to fix the two arbitrary functions of time $\xi(t, 0)$ and $\xi^0(t, 0)$, by requiring that $\xi(t, r_c)$ and

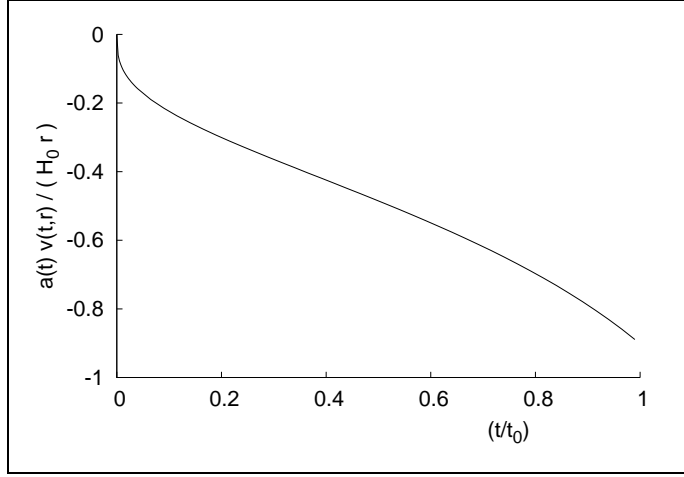


Figure 3: The quantity $a\tilde{v}/(H_0 r)$ in Region 1, plotted using parameter values from Table 1. Since $(H_0 r_*/c) \sim 0.001$, the peculiar velocity $a\tilde{v}$ remains small.

$\xi^0(t, r_c)$ vanish. This would be in line with the shell $r = r_c$ expanding like the flat EdS background. However, this complicates some of the expressions we evaluate, and does not change the order of magnitude of any of the final results. Hence we will continue to assume that the transformation functions ξ and ξ^0 vanish at $r = 0$ rather than at $r = r_c$. See also the end of Section 3.2.]

The peculiar velocity can be explicitly calculated to be

$$a(t)\tilde{v}(t, r) = (H_0 r) \left(\frac{\delta_*}{a_i} \right)^{1/2} \left[\frac{\sin u}{(1 - \cos u)} - \frac{2}{3} \frac{1 - \cos u}{(u - \sin u + B)} \right], \quad (42)$$

where the various functions are defined in Eqns. (18), and we have defined the constant B by

$$B \equiv \frac{2H_0 t_i}{1 + \delta_*} \left(\frac{\delta_*}{a_i} \right)^{3/2} - (u_i - \sin u_i). \quad (43)$$

In the rest of this section we will use the parameter values listed in Table 1. In Fig. 3 we have plotted $a\tilde{v}/(H_0 r)$ in Region 1. We see that this dimensionless quantity remains of order ~ 1 throughout the evolution. For our choice of $(H_0 r_*/c) \sim 10^{-3}$, which corresponds to an overdensity spanning a few Mpc today, the peculiar velocity is of order $\sim 10^{-3}$ in Region 1.

Knowing ξ and ξ^0 we can easily determine $\tilde{\psi}$ and \tilde{A} to be

$$\begin{aligned} \tilde{\psi} &= -\frac{1}{4} \left(\frac{\delta_*}{a_i} \right) (H_0 r)^2 - \frac{1}{2} a\tilde{v} R H \\ &= -\frac{1}{4} \left(\frac{\delta_*}{a_i} \right) (H_0 r)^2 \left[1 - \frac{4}{3} \left(\frac{2}{3} \frac{(1 - \cos u)^2}{(u - \sin u + B)^2} - \frac{\sin u}{(u - \sin u + B)} \right) \right], \\ &\equiv -\frac{1}{4} \left(\frac{\delta_*}{a_i} \right) (H_0 r)^2 f_1(u), \end{aligned} \quad (44)$$

$$\begin{aligned} \tilde{A} &= \frac{1}{4} \left(\frac{\delta_*}{a_i} \right) (H_0 r)^2 \left[\frac{4}{3} \left(2 \frac{\sin u}{u - \sin u + B} - \frac{(1 - \cos u)^2}{(u - \sin u + B)^2} \right) - 2 \frac{\cos u}{1 - \cos u} \right] + \frac{1}{2} (a\tilde{v})^2, \\ &\equiv \frac{1}{4} \left(\frac{\delta_*}{a_i} \right) (H_0 r)^2 f_2(u), \end{aligned} \quad (45)$$

where $a\tilde{v}$ is given in Eqn. (42), and the last equalities in the equations define the functions $f_1(u(t))$ and $f_2(u(t))$ respectively. In Fig. 4 we have plotted the functions $f_1(u(t))$ and $f_2(u(t))$.

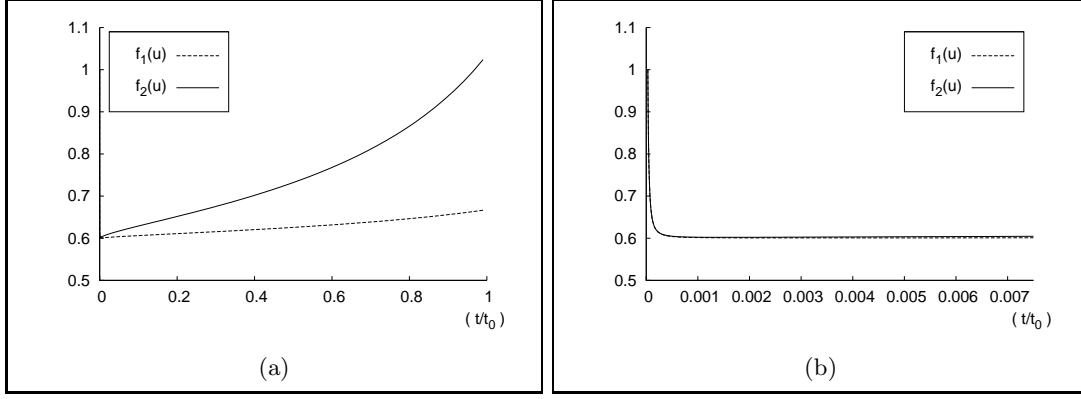


Figure 4: The time dependence of the functions $\tilde{\psi}$ and \tilde{A} in Region 1, using parameter values from Table 1. Panel (a) shows the evolution from t_i to t_0 , and panel (b) shows the early time evolution upto $t = 0.0075t_0$. The dotted lines correspond to $f_1(u(t))$ and the solid lines to $f_2(u(t))$ (see Eqns. (44) and (45) for definitions). We see that at early times, $\tilde{A} \simeq -\tilde{\psi}$. Since $(H_0 r_*/c) \sim 0.001$, $\tilde{\psi}$ and \tilde{A} remain small.

We see that they remain of order ~ 1 for most of the evolution, and hence for an overdensity spanning a few Mpc, $\tilde{\psi}$ and \tilde{A} are of order $\sim 10^{-6}$ in Region 1. By expanding $f_1(u)$ and $f_2(u)$ in the parameter u around its initial value u_i , one can show that at early times one has $\tilde{A} \simeq -\tilde{\psi}$, as expected in the linear theory. Fig. 4b shows this behaviour. However, the relative difference between \tilde{A} and $-\tilde{\psi}$ grows quickly and (for the parameters given in Table 1) becomes of the order 10^{-2} , by $t \sim 0.02t_0$. At the end of Section 3.2 we show that the large relative difference between \tilde{A} and $-\tilde{\psi}$ (of the order $\sim 50\%$ at late times), is largely due to our choice of setting these functions to zero at the origin. [We note that a difference between these two functions is not in principle surprising since the density contrast in Region 1 grows to order ~ 1 by $t \sim 0.3t_0$ (see Fig. 1a), and departures from the linear theory are expected to become significant even before this. See, however, Section 4 below.]

3.2 The transformation in Regions 2 and 3

The calculation in Regions 2 and 3 proceeds in a similar fashion as above, but in this case the integrals involved cannot be computed analytically. We will therefore display the expressions we obtain for \tilde{v} , ξ , and ξ^0 , and plot the results of numerically computing $\tilde{\psi}$ and \tilde{A} from these quantities.

- **Region 2** ($r_* < r < r_c$):

For numerical calculations we found it convenient to define the functions

$$B_1(r) \equiv \frac{1}{2} \frac{H_0^2}{a_i} r \left(\varepsilon - \frac{r\varepsilon'}{1+\varepsilon} \right), \quad (46a)$$

$$B_2(t, r) \equiv \frac{1}{2} \frac{H_0^2}{a_i} \frac{r^2 \varepsilon'}{(1+\varepsilon)} \frac{\varepsilon^{3/2}}{(1-\cos \alpha)^2} \left[H_i(t-t_i) \sin \alpha \frac{(3+\varepsilon)}{(1+\varepsilon)} + \frac{4\varepsilon^{1/2}}{(1+\varepsilon)^2} \frac{\sin \alpha}{\sin \alpha_i} \right], \quad (46b)$$

$$B_3(t, r) \equiv \frac{H_i \sin \alpha}{(1-\cos \alpha)^2} \frac{2\varepsilon^{3/2}}{1+\varepsilon}. \quad (46c)$$

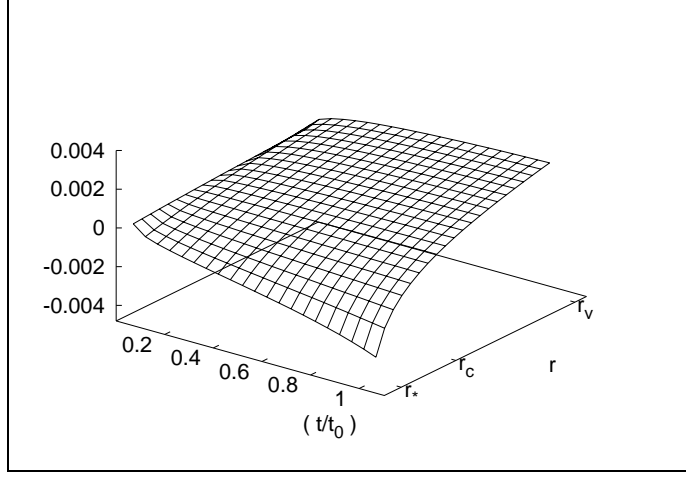


Figure 5: The peculiar velocity $a\tilde{v}/c$ in Regions 2 and 3 using parameter values from Table 1.

We then have

$$\xi(t, r) = \frac{1}{4} \left(\frac{\delta_*}{a_i} \right) (H_0 r_*)^2 + \int_{r_*}^r (B_1(\bar{r}) + B_2(t, \bar{r})) d\bar{r}, \quad (47)$$

$$\tilde{v} = \frac{R}{a} [B_3(t, r) - H], \quad (48)$$

$$\xi^0(t, r) = \xi^0(t, r_*) + a(t) \int_{r_*}^r \tilde{v}(t, \bar{r}) R'(t, \bar{r}) d\bar{r}, \quad (49)$$

where $\xi^0(t, r_*)$ is computed from Eqn. (41) at $r = r_*$. $\tilde{\psi}$ and \tilde{A} must now be computed using Eqns. (34) and (38) respectively. We have again used the `NIntegrate` routine of *Mathematica*.

• **Region 3** ($r_c < r < r_v$) :

The analysis is very similar to that in Region 2. We define the functions

$$D_1(r) \equiv \frac{1}{2} \frac{H_0^2}{a_i} r \left(\varepsilon - \frac{r\varepsilon'}{1+\varepsilon} \right), \quad (50a)$$

$$D_2(t, r) \equiv \frac{1}{2} \frac{H_0^2}{a_i} \frac{r^2 \varepsilon'}{(1+\varepsilon)} \frac{|\varepsilon|^{3/2}}{(\cosh \eta - 1)^2} \left[H_i(t - t_i) \sinh \eta \frac{(3+\varepsilon)}{(1+\varepsilon)} + \frac{4|\varepsilon|^{1/2}}{(1+\varepsilon)^2} \frac{\sinh \eta}{\sinh \eta_i} \right], \quad (50b)$$

$$D_3(t, r) \equiv \frac{H_i \sinh \eta}{(\cosh \eta - 1)^2} \frac{2|\varepsilon|^{3/2}}{1+\varepsilon}, \quad (50c)$$

and find

$$\xi(t, r) = \xi(t, r_c) + \int_{r_c}^r (D_1(\bar{r}) + D_2(t, \bar{r})) d\bar{r}, \quad (51)$$

$$\tilde{v} = \frac{R}{a} [D_3(t, r) - H], \quad (52)$$

$$\xi^0(t, r) = \xi^0(t, r_c) + a(t) \int_{r_c}^r \tilde{v}(t, \bar{r}) R'(t, \bar{r}) d\bar{r}, \quad (53)$$

where $\xi(t, r_c)$ and $\xi^0(t, r_c)$ are obtained from Eqns. (47) and (49) respectively, evaluated in the limit $r \rightarrow r_c^-$.

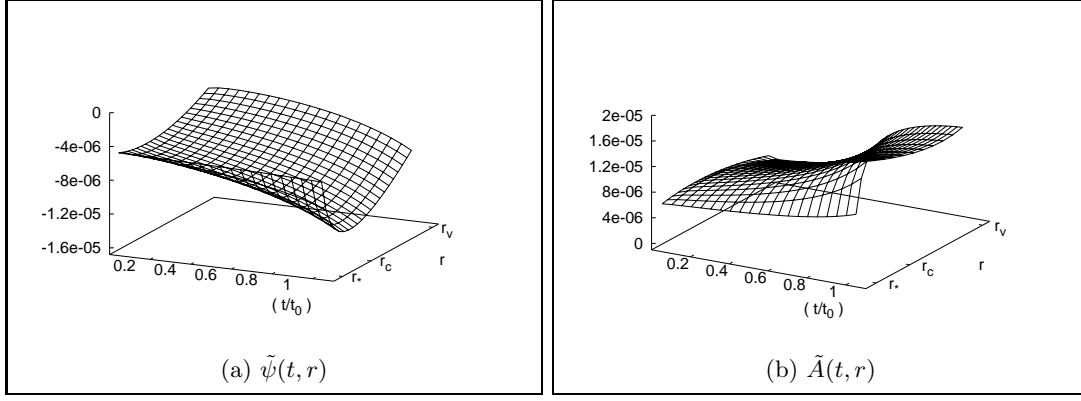


Figure 6: The metric functions $\tilde{\psi}(t, r)$ and $\tilde{A}(t, r)$ in Regions 2 and 3 using parameter values from Table 1. The time axis begins at $t = 50t_i$.

In Fig. 5, we have plotted the velocity $a\tilde{v}/c$ in Regions 2 and 3 for a range of time. It can be shown that at the order of approximation we are working at, $a\tilde{v}$ changes sign at $r = r_c$. [Recall $\varepsilon(r_c) = 0$ and hence this shell expands exactly like the EdS background. The metric in the (\tilde{t}, \tilde{r}) coordinates will not be exactly EdS at $r = r_c$, due to our unusual choice of normalisation for ξ and ξ^0 at $r = 0$. This does not pose any problem for our conclusions.]

In Fig. 6 we plot $\tilde{\psi}$ and \tilde{A} . We see that these functions are well behaved and remain small for the entire region of interest (in space and time). Hence the perturbed FLRW picture is indeed valid for this system, even though each region by itself appears to be very different from FLRW in the synchronous coordinates comoving with the matter. Due to numerical difficulties close to the initial time $t = t_i$, we have plotted the time axis starting from $t = 50t_i$.

Note that the magnitude of $\tilde{\psi}$ and \tilde{A} is sensitive to the overall size of the region, determined by the value of $R(t, r_v)$. For our parameter choices given in Table 1, the size of the region at the present epoch is $\sim 33\text{Mpc}$, which is a typical size for observed voids. The dependence is roughly $(HR)^2$, and hence a void which is about 10 times larger in length scale than the above value, would have metric functions about 100 times larger.

We end this subsection by noting two points. Firstly, we have seen that with our choices for certain arbitrary functions of time in Eqns. (40) and (41), the functions \tilde{A} and $-\tilde{\psi}$ build up a relative difference of $\sim 40\text{-}50\%$ by present epoch (see Figs. (4a) and (6)). However, it can be shown that if one redefines these functions so that they vanish at $r = r_c$ rather than at the origin (in line with the discussion below Eqn. (41)), then the relative difference between the functions reduces to $\sim 5\%$ at present epoch in Regions 2 and 3. This is demonstrated in Fig. 7 for two representative values of the coordinate r . In Region 1 the relative difference is maximum at the center $r = 0$, being about 30% at present epoch (which is obvious since with the redefined functions, the relative difference at the center is simply the relative difference of the *original* functions at $r = r_c$). The origin of the large relative difference seen in, e.g. Fig. 4a is therefore not completely clear, and may even be unphysical. This issue deserves more careful consideration, and we hope to return to it in future work (see also Section 4 below). In any case, we emphasize that our main result is that the magnitude of the functions \tilde{A} and $\tilde{\psi}$ themselves, is very small. This brings us to the second issue.

It is known that simply having a metric of the form (29) with only the *magnitude* of the perturbations being small, is not enough to guarantee consistency with Einstein's equations written as a perturbation series; additional constraints on the *derivatives* of these functions must be satisfied. These constraints, given in e.g. Ref. [8], take the form (for the metric (29)

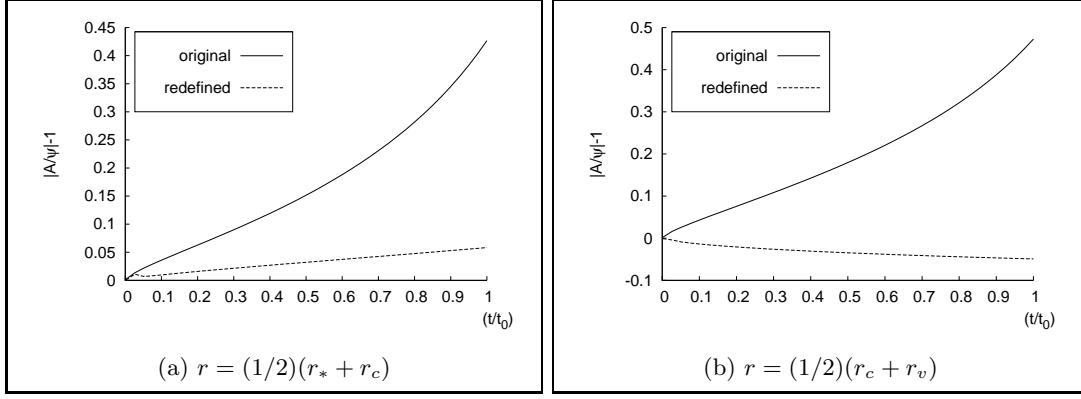


Figure 7: The relative difference between the metric functions \tilde{A} and $-\tilde{\psi}$, defined as $|\tilde{A}/\tilde{\psi}| - 1$, plotted as a function of time at $r = (1/2)(r_* + r_c)$ (panel (a)) and at $r = (1/2)(r_c + r_v)$ (panel (b)). The solid lines show the difference for the definition of the functions used in this paper. The dotted lines show the difference when the functions are redefined to vanish on $r = r_c$ instead of vanishing at the origin.

with $\tilde{\psi} = -\tilde{A}$,

$$\left| \frac{\partial \tilde{A}}{\partial t} \right|^2 \ll \frac{1}{a^2} \nabla^\alpha \tilde{A} \nabla_\alpha \tilde{A}, \quad \left(\nabla^\alpha \tilde{A} \nabla_\alpha \tilde{A} \right)^2 \ll \left(\nabla^\alpha \nabla^\beta \tilde{A} \right) \nabla_\alpha \nabla_\beta \tilde{A}, \quad (54)$$

where $\alpha, \beta = 1, 2, 3$, and ∇_α is the spatial covariant derivative associated with the flat 3-space metric. On dimensional grounds, treating $\tilde{A} \sim (HR)^2 \ll 1$, $\partial_t \sim H$ and $\nabla \sim aR^{-1}$, it is easy to see that these constraints will be satisfied by our solution. This should also be expected since we started from an exact solution of the Einstein equations and performed a self-consistent coordinate transformation.

3.3 The magnitude of the backreaction

One can now legitimately ask the question, “How large is the effect of the small metric inhomogeneities?” Naively, one would argue that small inhomogeneities must lead to small effects. Indeed, the question of the magnitude of the backreaction in the Newtonianly perturbed FLRW setting has been investigated by Behrend, *et al.* [10] in the linear and quasilinear regimes, and they find that corrections to the FLRW equations remain at the level of one part in 10^5 . The effect of perturbative metric inhomogeneities on observables such as the luminosity distance *evaluated using the perturbed FLRW metric with a fixed background*, has also been studied [11] and shown to be small. However, what we are dealing with is a situation in which the *matter* perturbations are completely nonlinear, and it is not *a priori* clear that the same arguments would carry through. Indeed, we saw in section 2 that the deceleration parameter q deviated from its EdS value by about $\sim 10\%$. Here we give an argument based on dimensional considerations supplemented with realistic numbers, which will show that this effect is scale dependent, and is not expected to be present if a sufficiently large averaging scale is chosen.

In the following we will work at the present epoch t_0 . Consider a model situation similar to the one we have been considering so far, such that at present epoch the physical extent of the overdense region is R_* , and that of the underdense is R_v . For order of magnitude estimates, we assume that in the perturbed FLRW metric (29) (which is valid for this system provided $H_0 R_v \ll 1$), $\tilde{A} \sim -\tilde{\psi}$. Also assume that the density contrast in the overdense region is δ_{*0} and that in the underdense region is δ_{v0} , where we take δ_{*0} and δ_{v0} to be constant in space, which is fine for an order of magnitude estimate. The backreaction in the Buchert approach contains, among other terms, the spatial average of the quantity $\nabla^2 \tilde{A}$ which appears in the

spatial curvature [6, 10], where ∇^2 is the Laplacian operator for the flat 3-space metric. The spatial curvature has the structure

$$\mathcal{R} \sim \frac{1}{a^2} \left[(\#_1) \nabla^2 \tilde{A} + (\#_2) \tilde{A} \nabla^2 \tilde{A} + (\#_3) (\nabla \tilde{A})^2 \right], \quad (55)$$

where $\#_1, \#_2, \#_3$ are constants whose values are irrelevant for this order of magnitude argument. Due to the Einstein equations in the small scale Newtonian approximation, the leading order effect in the *nonlinear* regime, comes from $\nabla^2 \tilde{A}$ which satisfies

$$\nabla^2 \tilde{A} \sim \begin{cases} H_0^2 \delta_{*0}, & \text{overdense region,} \\ H_0^2 \delta_{v0}, & \text{underdense region.} \end{cases} \quad (56)$$

Consider the situation when, at present epoch, $R_* \sim 6\text{Mpc}$, $R_v \sim 30\text{Mpc}$, $\delta_{*0} \sim 10^2$ and $\delta_{v0} \sim -0.9$. These are typical numbers for clusters of galaxies and voids. It is straightforward to now show that the spatial average of $\nabla^2 \tilde{A}$ over a domain comprising the overdense and underdense region, works out to be

$$\begin{aligned} \langle \nabla^2 \tilde{A} \rangle &\sim \frac{H_0^2}{R_*^3 + R_v^3} [R_*^3 \delta_{*0} + R_v^3 \delta_{v0}] , \\ &\simeq -0.1 H_0^2. \end{aligned} \quad (57)$$

It would appear therefore, that this spatial average of $\nabla^2 \tilde{A}$ (which is usually neglected) thus turns out to be a significant contributor to the backreaction. (In fact it is the most significant contributor, since the other terms are clearly of at least one higher order in the small quantity $(H_0 R_v)^2$, for such a model.)

As we now argue, however, the above effect can be deceptive, and is really scale dependent. Let the initial density contrasts in the overdense and underdense regions be δ_{*i} and δ_{vi} respectively, so that $\delta_{*i}, |\delta_{vi}| \ll 1$. If M_{*i} , M_{vi} , M_* and M_v are the masses at initial time and today, in the overdense and underdense region respectively, and ρ_i and ρ_0 are the values of the background density at initial time and today, then at initial time

$$M_{*i} \approx \rho_i (a_i R_*)^3 = \rho_0 R_*^3, \quad M_{vi} \approx \rho_0 R_v^3, \quad (58)$$

and at present time,

$$M_* = \rho_0 (1 + \delta_*) R_*^3 > M_{*i}, \quad M_v = \rho_0 (1 + \delta_v) R_v^3 < M_{vi}. \quad (59)$$

We now make the crucial observation that *if the averaging scale is large enough*, and we are counting several such “pairs” of overdense and underdense regions, then the mass ejected from the underdense region must have all gone into the overdense region. It is then easy to show, that

$$\delta_* R_*^3 \approx -\delta_v R_v^3, \quad (60)$$

which means that, just like in the linear theory, the average of $\nabla^2 \tilde{A}$ is expected to be negligible on such a scale. In the real universe, we do expect that the averaging scale must be at least of the order of the homogeneity scale, and on such a scale we will be sampling several pairs of overdense and underdense regions. The only cumulative effects that may arise with such a choice of scale are from terms such as $(\nabla \tilde{A})^2$, which as we mentioned earlier, are of one higher order in the perturbation and will give effects of the size $\sim H_0^2 (H_0 R_v)^2 \ll H_0^2$. (For a demonstration of the scale dependence of the effect, see e.g. the work of Li and Schwarz [14].)

In the light of this discussion, our results of section 2 (figures (2a)-(2c)) can be understood as arising due to the fact that we are not averaging on a scale large enough to sample many overdense and underdense pairs. In the language of the above argument, all the mass ejected

from the underdense region (in coordinates which are comoving with the *background*), is not going into the overdense region which is part of the averaging domain. Some of the matter is escaping outside the averaging domain and is left unaccounted for. This explains an imbalance as suggested by Eqn. (57).

4 Discussion

In this paper we have addressed the question of whether or not the assumptions involved in using a perturbed FLRW framework to describe the *metric* of the present Universe, break down during epochs of structure formation, and whether averaging over inhomogeneities in such a context can yield effects large enough to lead to an accelerating scale factor. We have demonstrated two things. First, it is very essential to impose initial conditions properly matched across any boundaries present in the model. Neglecting to do so (for example by ignoring certain regions such as Region 2 of our model) can lead to effects such as an accelerating effective scale factor a_{mod} . Also, as we saw in Fig. 2d, it *is* in principle possible to have very large deviations from FLRW-like conditions after averaging, but this is at the cost of initial conditions which are unrealistic when confronted with the CMB data.

Secondly, we have shown that, provided peculiar velocities of matter are small (which is a reasonable assumption on observational grounds), one can explicitly find coordinates in which the metric of the Universe is of the perturbed FLRW form (29). This by itself is not a surprising result, since one can always do this locally (our Region 1 for example is a closed FLRW sub-Universe by itself, without any coordinate transformations). What is important is the fact that the background FLRW used for comparison is taken to be uniquely and *globally* defined, so that *every* local region involved in structure formation can be compared to this background in an unambiguous fashion. The existence of this global FLRW model is not simply an assumption made at the present epoch, it is justified by the fact that density fluctuations in the *past* were very small.

An issue worth highlighting again is that the time coordinates involved in the transformation from the synchronous coordinates to the perturbed FLRW form, are linked by an infinitesimal transformation (after controlling some degrees of freedom by setting arbitrary functions of time to zero), as expected with weak gravitational fields. While our model is perhaps not the most realistic depiction of observed voids, we expect this feature to hold in more realistic models also. At first glance this may appear to differ from Wiltshire's claim [4] that the clocks of observers in bound regions face a significant calibration when compared with those inside large voids. However the issue is rather subtle, since Wiltshire's arguments involve a different choice of time slicing than the standard constant t hypersurfaces used here, and his model shows cumulative effects over large times. It is possible that these cumulative effects are related to the relative difference between the metric functions which we discussed in Section 3, but a straightforward comparison is not possible at this stage. In this context, it becomes essential to understand the origins of those differences, and moreover the fact that the magnitude of the difference is sensitive to boundary conditions.

A few remarks concerning further tests of the backreaction argument, with more realistic models of structure formation which should account for pressure. We have not modelled voids *surrounded* by overdensities, since such models are plagued by shell-crossings in the absence of pressure. (Our current model also faces this difficulty beyond region 3.) But qualitatively, we expect our results to hold even in models where a suitable pressure term takes care of shell crossings and leads to stable structures surrounding expanding voids, since we expect peculiar velocities to remain small in this situation as well. As long as the sizes of individual voids are not an appreciable fraction of the Hubble scale, one expects that here as well, it will be possible to find coordinate transformations like the one we have presented. We will return to

this problem in future work.

Finally, we comment on an issue which deserves careful consideration. Recall that in the Buchert scheme of averaging perturbative inhomogeneities, which has been employed by several authors [3, 10, 13], there are *two* scale factors – the background scale factor $a(t)$ which satisfies the usual FLRW equations, and the effective scale factor $a_D(t)$ which satisfies the Buchert equations [6]. It is our belief that this situation has an inherent ambiguity – which of the two scale factors is relevant for observations? In our opinion, a more consistent way of proceeding would be to employ the fully covariant averaging scheme due to Zalaletdinov [7], developed further in the cosmological context by [21]. In this scheme, there would be only *one* scale factor, unambiguously associated with a background metric, which would satisfy the *corrected* Einstein equations. The fact that backreaction is negligible in the linear regime should allow the problem to be well-posed at say the last scattering epoch. While we have estimated the effects of averaging inhomogeneities to be negligible on large enough scales in Buchert’s scheme, this was done in a perturbation theory around the *fixed* Einstein-deSitter background. It is not clear that this result will continue to hold even at late times when the background itself is “evolving”, namely, being corrected by the (small but cumulative) effects of inhomogeneities. Note that *if* these effects build up at late times, then in this scheme with only one scale factor, the evolution of the perturbations will also be modified, which may lead to some interesting effects. We will investigate these issues in the near future.

In conclusion, we wish to suggest that it has not yet been conclusively established that cosmological backreaction becomes large enough during the structure formation phase to cause an acceleration of the scale factor. On the contrary, the calculation presented in the present paper suggests that the backreaction remains small during this phase, and that the intuitive picture concerning weak gravitational fields is actually realized in the form of a perturbed FLRW metric. Self-consistently accounting for the effects that the backreaction would implicitly have on the evolution of the perturbations (via the scale factor), may lead to interesting effects which remain to be explored.

Acknowledgments : It is a pleasure to thank Karel van Acoleyen and T. Padmanabhan for several useful discussions. We are also grateful to Thomas Buchert, Syksy Räsänen, Dominik Schwarz and David Wiltshire for their critical comments on an earlier draft.

References

- [1] S Räsänen, *JCAP* 0611:003, (2006) [arXiv:astro-ph/0607626].
- [2] T Buchert, arXiv:0707.2153[gr-qc], to appear in Gen. Rel. Grav. (2008);
G M Hossain, arXiv:0709.3490[astro-ph], (2007);
A Paranjape and T P Singh, *Class. Quant. Grav.* **23**, 6955, (2006) [arXiv:astro-ph/0605195].
- [3] E W Kolb, S Matarrese and A Riotto, *New J. Phys.* **8**, 322, (2006) [arXiv:astro-ph/0506534];
A Notari, *Mod. Phys. Lett.* **A21**, 2997, (2006) [arXiv:astro-ph/0503715].
- [4] D L Wiltshire, *New J. Phys.* **9**, 377, (2007) [arXiv:gr-qc/0702082]; *Phys. Rev. Lett.* **99**, 251101, (2007) [arXiv:0709.0732[gr-qc]];
B M Leith, S C C Ng and D L Wiltshire, *Astrophys. J.* **672**, L91, (2008) [arXiv:0709.2535[astro-ph]].
- [5] G F R Ellis, in *General Relativity and Gravitation* (D. Reidel Publishing Co., Dordrecht), Eds. B. Bertotti et al., (1984).

- [6] T Buchert, *Gen. Rel. Grav.* **32**, 105, (2000) [arXiv:gr-qc/9906015]; *Gen. Rel. Grav.* **33**, 1381, (2000) [arXiv:gr-qc/0102049].
- [7] R M Zalaletdinov, *Gen. Rel. Grav.* **24**, 1015, (1992); *Gen. Rel. Grav.* **25**, 673, (1993).
- [8] A Ishibashi and R M Wald, *Class. Quant. Grav.* **23**, 235, (2006) [arXiv:gr-qc/0509108].
- [9] C Wetterich, *Phys. Rev.* **D67**, 043513, (2003) [arXiv:astro-ph/0111166].
- [10] J Behrend, I A Brown and G Robbers, arXiv:0710.4964[astro-ph], (2007), to appear in JCAP.
- [11] R A Vanderveld, E E Flanagan and I Wasserman, *Phys. Rev.* **D76**, 083504, (2007) [arXiv:0706.1931 [astro-ph]].
- [12] T Buchert, M Kerscher and C Sicka, *Phys. Rev.* **D62**, 043525, (2000) [arXiv:astro-ph/9912347].
- [13] N Li and D Schwarz, *Phys. Rev.* **D76**, 083011, (2007) [arXiv:gr-qc/0702043].
- [14] N Li and D Schwarz, arXiv:0710.5073[astro-ph], (2007).
- [15] F Hoyle and M S Vogeley, *Astrophys. J.* **566**, 641, (2002) [arXiv:astro-ph/0109357]; *Astrophys. J.* **607**, 751, (2004) [arXiv:astro-ph/0312533];
M S Vogeley *et al.*, in *Proceedings IAU Colloquium No. 195*, (2004), A. Diaferio, ed.;
S G Patiri, *et al.*, *Mon. Not. R. Astr. Soc.* **369**, 335, (2006) [arXiv:astro-ph/0506668];
K Tomita, *Mon. Not. R. Astr. Soc.* **326**, 287, (2001) [arXiv:astro-ph/0011484]; *Prog. Theor. Phys.* **106**, 929, (2001) [arXiv:astro-ph/0104141];
A V Tikhonov and I D Karachentsev, *Astrophys. J.* **653**, 969, (2006) [arXiv:astro-ph/0609109].
- [16] For a Newtonian treatment of shell crossings in spherical collapse, see e.g. –
E Bertschinger, *Astrophys. J. S.* **58**, 1, (1985); *Astrophys. J. S.*, **58**, 39, (1985);
G L Hoffman, D W Olson and E E Salpeter, *Astrophys. J.* **242**, 861, (1980).
M A Sanchez-Conde, J Betancort-Rijo and F Prada, *Mon. Not. R. Astron. Soc.* **378**, 339, (2007) [arXiv:astro-ph/0609479].
See also
K Bolejko, A Krasinski and C Hellaby, *Mon. Not. R. Astron. Soc.* **362**, 213, (2005) [arXiv:gr-qc/0411126];
R K Sheth and R van de Weygaert, *Mon. Not. R. Astron. Soc.* **350**, 517, (2004) [arXiv:astro-ph/0311260].
- [17] G Lemaître, *Ann. Soc. Sci. Brux.* **A53**, 51, (1933) (in French)
G Lemaître, *Gen. Rel. Grav.* **29**, 5, (1997) (reprint).
R C Tolman, *Proc. Nat. Acad. Sci* **20**, 169, (1934).
H Bondi, *Mon. Not. R. Astron. Soc.* **107**, 410, (1947).
- [18] T Padmanabhan, *Structure Formation in the Universe*, Cambridge Univ. Press, (1993);
A Krasinski, *Inhomogeneous Cosmological Models*, Cambridge Univ. Press, (1997);
A Krasinski and C Hellaby, *Phys. Rev.* **D65**, 023501, (2002) [arXiv:gr-qc/0106096];
C Hellaby and A Krasinski, *Phys. Rev.* **D73**, 023518, (2006) [arXiv:gr-qc/0510093].
- [19] S Dodelson, *Modern Cosmology*, Academic Press, (2003).
- [20] M Malekjani, S Rahvar and D M Z Jassur, arXiv:0706.3773[astro-ph], (2007).
- [21] A Paranjape and T P Singh, *Phys. Rev.* **D76**, 044006, (2007) [arXiv:gr-qc/0703106].